

Cost effective nanofiber composite membranes for Cr(VI) adsorption with high durability

*Dandan Xu, Shan Yan, Weng Wei, Ru Xiao**

State Key Laboratory for Modification of Chemical Fibers and Polymer Materials, College of Materials Science and
Engineering, Donghua University, Shanghai 201620, P. R. China

E-mail address: xiaoru@dhu.edu.cn (Ru Xiao)

1. Analysis of EVOH nanofibers

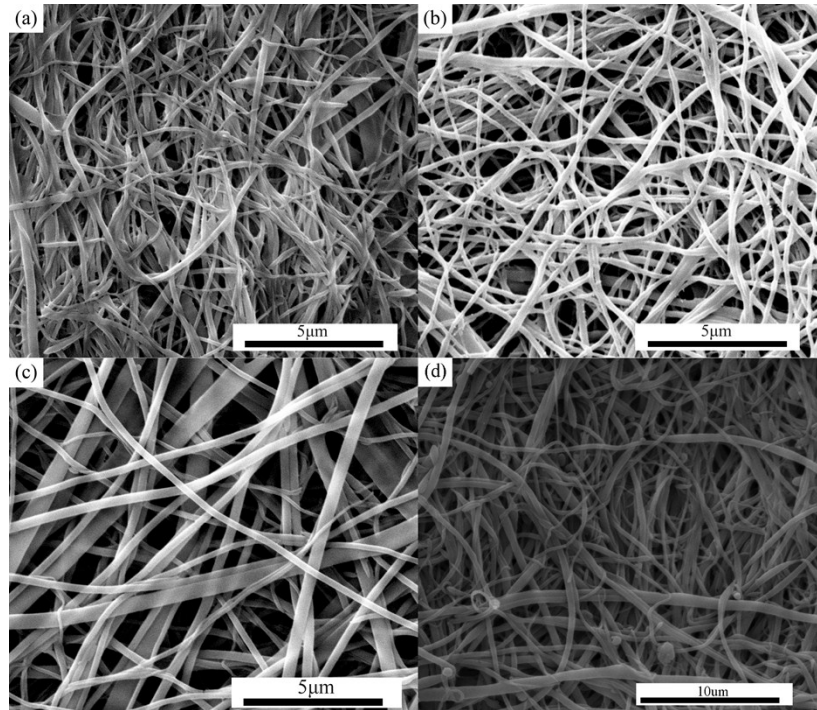


Fig. E1. The SEM image of EVOH nanofibers with different blend ratios: (a) 10/90, (b) 15/85, (c) 20/80, (d) 25/75.

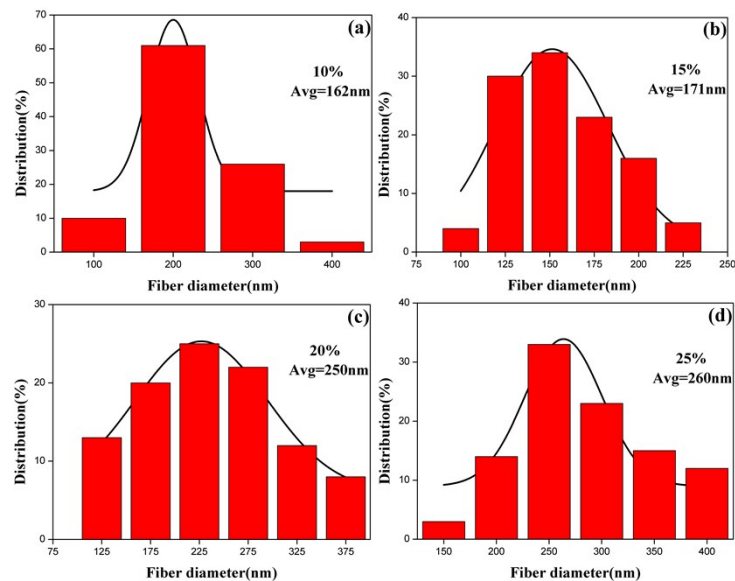


Fig. E2. Diameter distribution of EVOH nanofibers with different blend ratio: (a) 10/90, (b) 15/85, (c) 20/80, (d) 25/75.

Fig. E1 shows the SEM image of EVOH nanofibers with different blend ratio, at the blend ratios of EVOH/CAB 10/90, 15/85, 20/80, 25/75, EVOH nanofibers could be obtained after removal of the CAB matrix. The surface morphology of EVOH nanofibers was regular and smooth. Fig. E2 shows the diameter distribution of EVOH nanofibers with different blend ratio. With the increasing of EVOH percentage, the average diameter of EVOH naofibers increased and diameter distribution widened. With EVOH percentage ranged from 10 to 25wt%, the average diameter of EVOH nanofibers were 162, 171, 250, 260 nm, respectively.

2 The specific surface area of EVOH nanofibers and PECNM

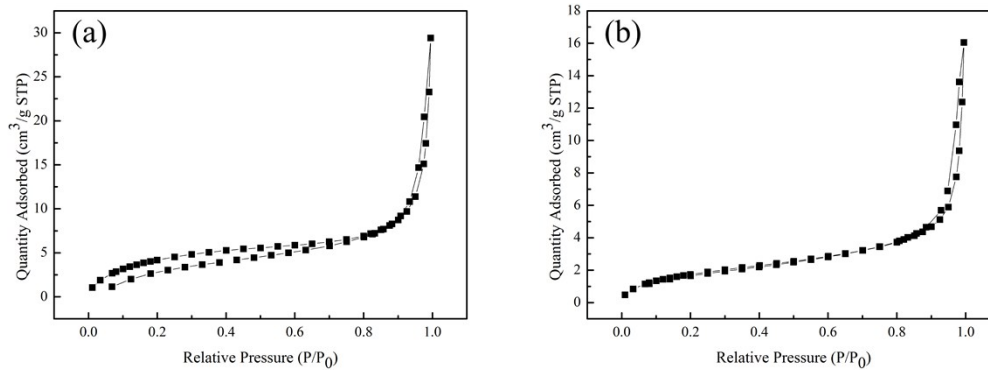


Fig. E3. Nitrogen adsorption-desorption isotherm of EVOH nanofibers (a) and PECNM (b)

Table E1 The Surface Area and Pore Properties Date of Nanofiber Membranes.

Nanofibrous Membrane	$SA_{BET}^a/(m^2 \cdot g^{-1})$	PD_{BJH}^b/nm
EVOH	16.1038	11.2958
EVOH/PANI	6.6821	14.8538

3 Effect of ionic strength

Chloride is the most predominant anion in aqueous systems, making it a priority for study during the adsorption of Cr(VI). In this investigation, NaCl was chosen to study the

effect of background ionic strength on the adsorption of Cr(VI). A series of experiments with the same initial Cr(VI) concentration of 100 mg/L at pH 2.0 and the ionic strengths were adjusted by NaCl at 30 °C were carried out. As illustrated from Fig. E4, the adsorption capacity of Cr(VI) slightly reduced with the increase of chloride ion concentration within the experimental range and still remains 92% of that without NaCl. These results reveal that the high selectivity of PECNM toward Cr(VI) was affected slightly by the presence of chloride ions. This phenomenon can be attributed to the following reasons: competition of Cl⁻ with Cr(VI) for the adsorption sites on PECNM results in the decrease of the adsorption capacity, at the same time, Cl⁻ and Na⁺ were monovalent anions, they could not or slightly compete for the adsorption site of PECNM at low concentration.

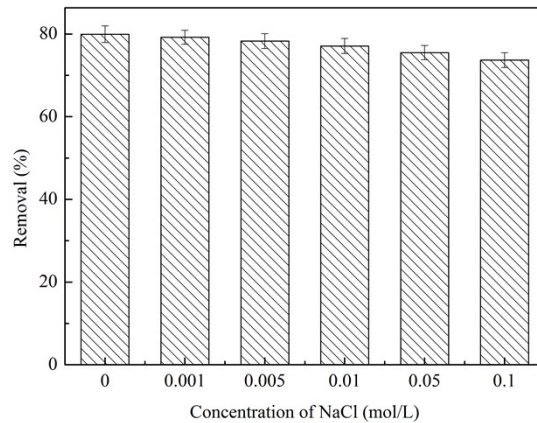


Fig. E4. Effect of ionic strength on adsorption of Cr(VI).

4 Adsorption Kinetics

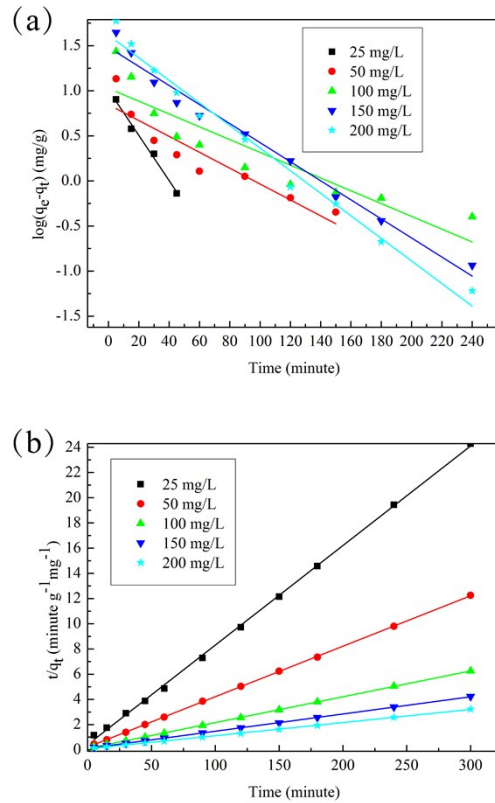


Fig. E5. (a) Pseudo-first-order kinetic model, (b) pseudo-second-order kinetic model for Cr(VI) adsorption on PECNM.

The linear forms can be formulated as equations (10) and (11), respectively:

$$\log(q_e - q_t) = \log q_e - \frac{K_1}{2.303} t \quad (1)$$

$$\frac{t}{q_t} = \frac{1}{K_2 q_e^2} + \frac{1}{q_e} t \quad (2)$$

where K_1 is the equilibrium rate constants of pseudo-first order, K_2 is the equilibrium rate constants of pseudo-second order. The kinetic data were treated using these two models and the parameters including rate constants K_1 , K_2 and correlation coefficients were calculated and the results were presented in Fig. E5 and Table E2. The correlation coefficients obtained by pseudo-first-order ($R^2 \approx 0.81523-0.98526$) are smaller than by pseudo-second-order ($R^2 \approx 0.99926-0.99991$), which is closer to 1 and the equilibrium adsorption capacities ($q_{e,c}$) calculated by pseudo-second-order are close to the

experimental q_e . This indicated that the pseudo-second-order model can better describe the Cr(VI) adsorption process compared to pseudo-first-order model, which suggests that the adsorption process may be a chemical adsorption process with electrostatic interaction and exchange of electrons between PECNM and adsorbates. It is worth noting that the value of K_2 decreased as the initial concentration increased, which means that the lower the initial concentration of Cr(VI) in the adsorption solution, the greater probability for Cr(VI) to bond to active sites on the absorbent.

Table E2 Kinetic parameters obtained from Lagergren pseudo-first-order and pseudo-second-order for Cr(VI) adsorption

C_0 (mg/L)	$q_{e,exp}$ (mg/g)	Pseudo-first-order			Pseudo-second-order		
		K_1 (L/min)	$q_{e,cal}$ (mg/g)	R^2	K_2 (g/mg·min)	$q_{e,cal}$ (mg/g)	R^2
25	12.35	5.78×10^{-2}	10.15	0.98526	1.543×10^{-2}	12.66	0.99926
50	24.49	2.03×10^{-2}	7.02	0.84955	7.7169×10^{-3}	24.98	0.99991
100	47.97	1.64×10^{-2}	10.61	0.81523	3.963×10^{-3}	48.78	0.99988
150	70.94	2.43×10^{-2}	30.29	0.97882	1.816×10^{-3}	73.10	0.99984
200	93.09	2.88×10^{-2}	41.31	0.98084	1.485×10^{-3}	95.97	0.99969

5 Adsorption Isotherms

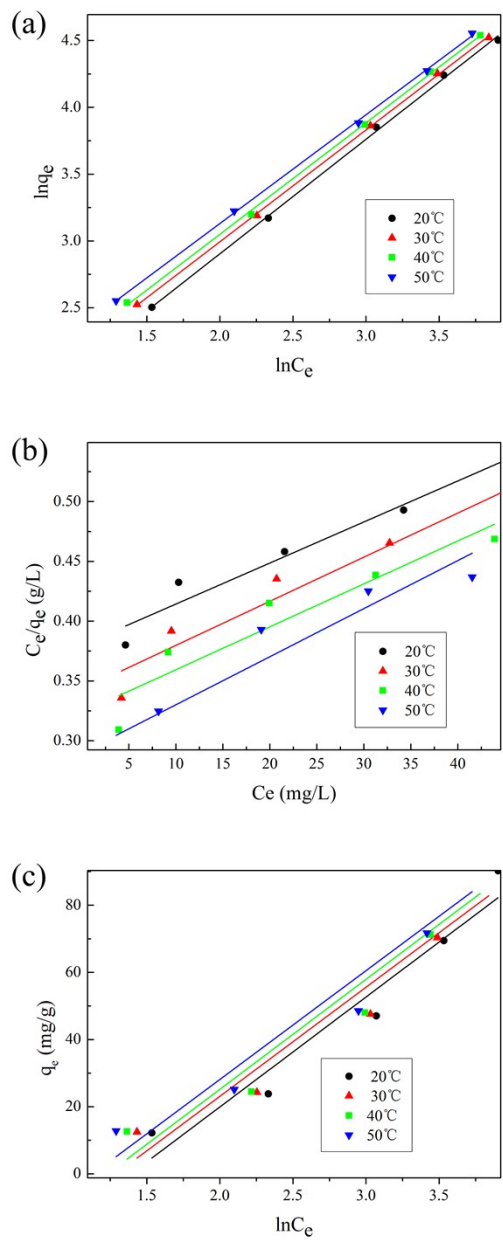


Fig. E6. (a) Freundlich isotherm model, (b) Langmuir isotherm model and (c) Temkin isotherm model for Cr(VI) adsorption on PECNM.

The Freundlich model is often used to describe the adsorption process on a heterogeneous surface of an adsorbent. The Langmuir model is used to describe the adsorption on a homogeneous and flat surface of an adsorbent, and each adsorptive site could be occupied only once in a one-on-one manner.

The linear isotherm equations are expressed as follows [Eqs. (3), (4), (5) and (6)]:

$$\text{Freundlich: } \ln q_e = \ln k_f + \frac{\ln C_e}{n} \quad (3)$$

$$\text{Langmuir: } \frac{C_e}{q_e} = \frac{1}{q_m d} + \frac{C_e}{q_m} \quad (4)$$

$$\text{Temkin: } q_e = \frac{RT}{b} \ln A + \frac{RT}{b} \ln C_e \quad (5)$$

$$\frac{RT}{b} = B \quad (6)$$

where k_f and n are the Freundlich empirical constants; q_m denotes the maximal adsorption capacities (mg/g), d is the Langmuir constant related to adsorption rate constant (L/mg); A and B are the Temkin constants. Data analyzed from the plots shown in Fig. E6 and listed in Table E3.

Table E3 Freundlich, Langmuir and Temkin parameters for Cr(VI) adsorption

Temp (°C)	Freundlich model			Langmuir model			Temkin model		
	Kf (mg/g)	1/n	R ²	q _m (mg/g)	b L/mg	R ²	B (J/mol)	A (L/mg)	R ²
20°C	3.2846	0.8572	0.99859	291.55	9.026×10 ⁻³	0.95207	32.7281	0.2487	0.92467
30°C	3.7386	0.8372	0.99969	271.00	10.762×10 ⁻³	0.91866	32.4683	0.2755	0.91306
40°C	3.973	0.8348	0.99924	278.55	11.098×10 ⁻³	0.85419	32.7363	0.2919	0.90146
50°C	4.489	0.8142	0.99947	248.76	13.867×10 ⁻³	0.87084	32.3900	0.3223	0.90223

6 PECNM after adsorption

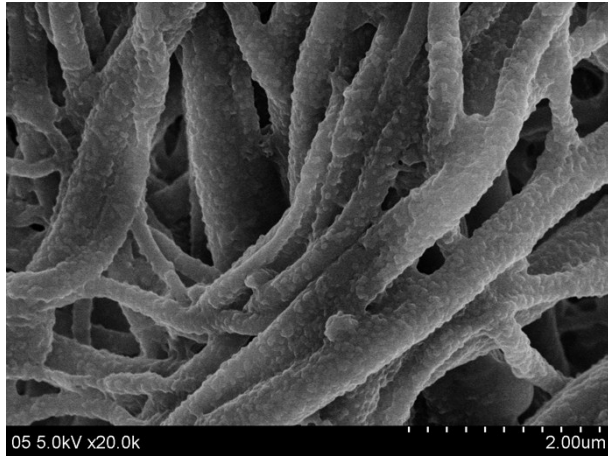


Fig. E7. FESEM image of PECNM after five times adsorption.